Atmospheric pCO$_2$ and depositional environment from stable-isotope geochemistry of calcrete nodules (Barremian, Lower Cretaceous, Wealden Beds, England)

STUART A. ROBINSON[1], JULIAN E. ANDREWS[2], STEPHEN P. HESSELBO[1],
JONATHAN D. RADLEY[3,4], PAUL F. DENNIS[2], IAN C. HARDING[5] & PERCE ALLEN[6]

[1]*Department of Earth Sciences, University of Oxford, Parks Road, Oxford OX1 3PR, UK*
(e-mail: stuartr@earth.ox.ac.uk)

[2]*School of Environmental Sciences, University of East Anglia, Norwich NR4 7TJ, UK*

[3]*Palaeobiology Research Group, School of Earth, Environmental and Physical Sciences, University of Portsmouth PO1 3QL, UK*

[4]*The Warwickshire Museum, Market Place, Warwick CV34 4SA, UK*

[5]*School of Ocean and Earth Science, University of Southampton, Southampton Oceanography Centre, European Way, Southampton SO14 3ZH, UK*

[6]*PRIS, University of Reading, Reading RG6 6AB, UK*

Abstract: Nodular soil carbonates (calcretes) are present in overbank facies of Lower Cretaceous, non-marine Wealden Beds (Wessex Formation) of southern England. Field evidence suggests that these calcretes formed mostly under semi-arid Mediterranean-type climatic conditions. Typical calcrete fabrics, identified petrographically, include floating detrital grains, corroded grain margins and circumgranular cracks defining peds. Localized alteration of primary micrites is mainly associated with large cracks where early non-ferroan diagenetic cementation and neomorphism was focused. Diagenetic ferroan calcites occur as void fills and yield relatively light carbon-isotope and oxygen-isotope compositions (δ^{13}C= $-15.0‰$; δ^{18}O= $-6.3‰$) compared to well-preserved micrite (δ^{13}C= $-10.2‰$; δ^{18}O= $-4.0‰$). Precise definition of δ^{13}C values for well-preserved micrites allow estimation of partial pressure of atmospheric CO$_2$ (pCO$_2$) for the early Barremian of 560 ppmV using a published diffusion-reaction model. The data suggest that atmospheric CO$_2$ was low during the mid-Early Cretaceous before rising to a previously defined mid-Cretaceous high. Data from calcretes in the Weald Clay highlight the need for selection of appropriate material and careful evaluation before pCO$_2$ calculations are attempted. The Weald Clay samples come from marshy palaeoenvironments where ingress of atmospheric CO$_2$ into the soil-zone was either reduced or prevented.

Keywords: Early Cretaceous, calcrete, palaeoatmosphere, carbon dioxide, stable isotopes.

The Early Cretaceous was a period of large-scale fluctuation in the isotopic composition of both the marine and terrestrial carbon reservoirs (e.g. Weissert & Bréhéret 1991; Lini *et al.* 1992; Hasegawa 1997; Menegatti *et al.* 1998; Gröcke *et al.* 1999). Over short periods of time, perturbations in the global carbon cycle reflected by the isotopic data probably had a significant affect on the amount of carbon dioxide present in the Early Cretaceous atmosphere (Lini *et al.* 1992; Gröcke *et al.* 1999; Jenkyns 1999). In addition, the Early Cretaceous is thought to have been a time of elevated partial pressure of atmospheric CO$_2$ (pCO$_2$), which was possibly related to increased rates of mid-ocean ridge spreading and associated volcanism (e.g. Jones & Jenkyns 2001). In order to study palaeoenvironmental conditions within the so-called 'Cretaceous Greenhouse' (e.g. Spicer & Corfield 1992; Larson & Erba 1999) it is desirable to have a detailed record of atmospheric pCO$_2$ change through time.

During the last decade the δ^{13}C of soil carbonate has been used as a proxy for estimating palaeoatmospheric pCO$_2$ in pre-Miocene times (e.g. Cerling 1991, 1992, 1999; Andrews *et al.* 1995; Mora *et al.* 1996; Ekart *et al.* 1999). These estimates have all been made using versions of Cerling's (1984, 1991, 1992, 1999) diffusion model where the δ^{13}C of pristine soil carbonate is key. Use of the Cerling model provides a method to verify the values predicted from long-term carbon-cycle models (e.g. Berner 1991, 1994; Tajika 1999; Wallmann 2001). The present study focuses on Lower Cretaceous (Wealden) palaeosols from southern England, providing new data to help assess the variability of atmospheric pCO$_2$ through the Cretaceous as a whole.

Geological setting

During the Early Cretaceous, non-marine Wealden sediments were deposited across much of what is now southern England. These sediments comprise variegated sandstones and mudstones of fluvial and lagoonal origin (Allen 1975, 1981). Two stratigraphic schemes exist for the English onshore Wealden strata: one for the Weald area and another for the Isle of Wight and Dorset (Figs 1 and 2; Allen & Wimbledon 1991). In the Weald, the cyclic alluvial and lagoonal sediments of the Hastings Beds (formally a group within the Wealden Supergroup in the Weald area) give way to the dominantly lacustrine-lagoonal sediments of the Weald Clay (formally a group) at approximately the Valanginian-Hauterivian

Age (Ma)		Stage	Isle of Wight & Dorset	Weald
	Early Cretaceous	Aptian	Lower Greensand Group	Lower Greensand Group
124.5				- - - ? - - -
		Barremian	Vectis Fm	Weald Clay Group
			- - ? - -	
132.0				
		Hauterivian	Wessex Fm	
135.0				
		Valanginian		Hastings Beds Group
140.5				
		Berriasian	Purbeck Group	Purbeck Group
145.5				

(WEALDEN BEDS spanning Vectis Fm/Wessex Fm column; WEALDEN BEDS spanning Weald column)

Fig. 1. Generalized stratigraphic column for the onshore Lower Cretaceous of southern England. Lithostratigraphy based upon Allen & Wimbledon (1991). Time scale from Harland *et al.* (1990).

Fig. 2. (a) Map of southern England and Wales. **(b)** Map of SE England showing the onshore outcrop of Wealden sediments and the position of Ockley, Swanage Bay and the Isle of Wight. **(c)** Detailed map of the SW coast of the Isle of Wight showing various localities that are discussed in the text (details in Table 1).

boundary. On the Isle of Wight and in parts of Dorset, the alluvial facies of the Wessex Formation of Early Barremian age are succeeded by the younger Vectis Formation (dominantly lacustrine-lagoonal) of mid-Barremian age.

The alluvial facies of the Wessex Formation can be divided into channel and overbank facies. The floodplain sediments (sheet sandstones, green-grey mudstones, mottled mudstones and red mudstones) have been interpreted as the deposits of a seasonal wetland catena (Wright *et al.* 2000) that resulted from variations in alluvial topography and seasonal flooding. Within the red mudstones of the Wessex Formation pseudo-anticlines, calcrete nodules and peds have been recognized (Wright *et al.* 2000).

The present study is based on calcrete nodules from (1) Wessex Formation localities on the Isle of Wight (Fig. 2) and at Swanage in Dorset (Fig. 2) and (2) from the Upper Weald Clay at Ockley Smokejacks Brickworks in Surrey (Fig. 2). Full locality details are given in Table 1. As for the exposed Wessex Formation on the Isle of Wight, the Upper Weald Clay of the Weald is thought to be of Early Barremian age (Allen & Wimbledon 1991). Correlation between the Swanage locality and the Isle of Wight is problematic, but palynological and palaeobotanical work suggests that the Swanage samples may be Late Hauterivian (see Hughes & Croxton 1973; Oldham 1976).

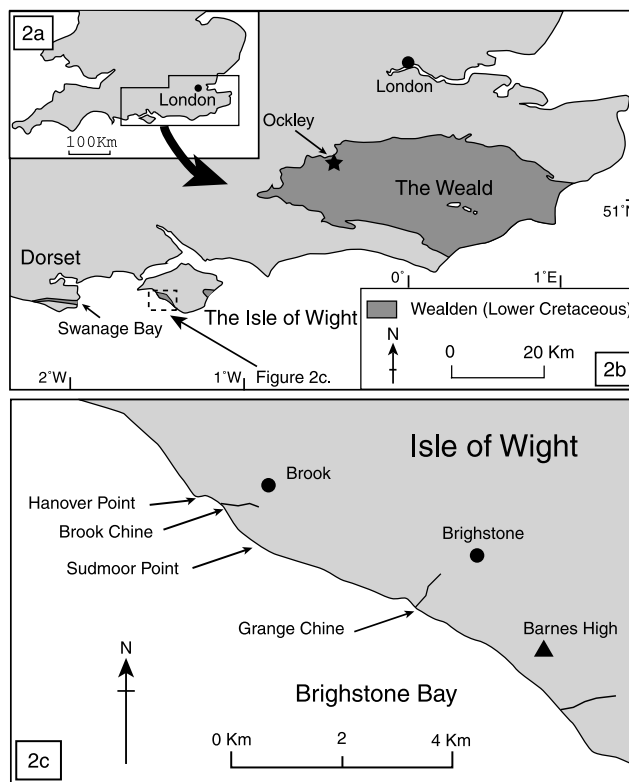The calcrete nodules are typically less than 100 mm across, greenish/pale grey with red mottles and occur in discrete horizons, as would be expected on a low-carbonate alluvial plain (Allen 1998) or reworked into channel lags. *In situ* nodules come principally from the red mudstones with pseudoanticlines, interpreted as vertisols by Wright *et al.* (2000). The Upper Weald Clay at Ockley represents mainly lacustrine deposits (Batten 1998). However, the peds and nodules come from slikensided varicoloured clays, suggesting a poorly-developed lake-margin or lagoon-margin vertisol.

Methods

The calcrete nodules described and analysed in this study were all collected from *in situ* positions within soil profiles. Pedogenic and diagenetic fabrics were observed from hand specimen cut slabs, standard thin sections and polished thin sections. Cathodoluminescence (CL) analysis of thin sections was by means of a cold cathode Technosyn instrument run at accelerating voltage of 18-20 kV and a gun current of 180–200 μA. For standard optical microscopy, thin sections were stained with combined alizarin red S and potassium ferricyanide after the method of Dickson (1965) to clarify fabrics and define ferroan and non-ferroan carbonate. For isotopic analysis sub-samples of 2–5 mg were drilled every 2–3 mm where possible, along transects on cut surfaces (Oxford), or from clearly defined fabrics such as pure micrites and spar-filled veins (UEA). Organic matter was removed by a 10% H_2O_2 leach (Oxford) or by low temperature plasma ashing (UEA). The samples were then processed using normal laboratory procedures and measured on a VG Prism mass spectrometer (Oxford) and on a Sira Series II mass spectrometer (UEA). Isotopic data are reported in delta notation relative to the Vienna Pee Dee Belemnite (VPDB) international scale (Coplen 1994). The mass spectrometers were calibrated using the NBS 18 and NBS 19 standards. Isotopic data for random samples were

Table 1. *Summary of all the data discussed in this paper*

Geology	Locality [National Grid Reference]	Sample code	Carbonate type	Average δ^{13}C (VPDB, ‰)	Average δ^{18}O (VPDB, ‰)
Wessex Formation (Upper Hauterivian?)	Swanage Bay, Dorset *c.* 90 m above the Arkell's (1947) Coarse Quartz Grit [SZ 034 802]	21999a	Well-preserved micrite	–9.1	–2.2
Wessex Formation (Lower Barremian)	South of Brook Bay, IOW *c.* 3 m below Sudmoor Point Sst [SZ 390 828]	SP1	Well-preserved micrite	–10.1	–4.1
			Mixed micrite	–10.4	–4.1
		SP1a	Well-preserved micrite	–10.3	–3.9
			Mixed micrite	–10.1	–4.0
Wessex Formation (Lower Barremian)	Chilton Chine, IOW *c.* 2 m above Sudmoor Point Sst. [SZ 408 822]	X20	Well-preserved micrite	–10.3	–4.3
			Spar	–14.2	–6.3
Wessex Formation (Lower Barremian)	SE of Chilton Chine, IOW 20 m above Sudmoor Point Sst [SZ 411 820]	W1	Well-preserved micrite	–10.6	–4.6
Wessex Formation (Lower Barremian)	Brighstone Bay, IOW Base of the Brighstone Sst [SZ 415 819]	W3	Well-preserved micrite	–9.1	–4.0
Wessex Formation (Lower Barremian)	Brighstone Bay, IOW *c.* 2 m above the Brighstone Sst [SZ 415 819]	GC2a	Well-preserved micrite	–9.7	–3.3
		GC2b	Mixed micrite	–9.7	–3.5
			Well-preserved micrite	–10.5	–4.3
			Mixed micrite	–9.8	–3.7
			Well-preserved micrite	–10.5	–4.2
			Mixed micrite	–9.7	–3.7
			Spar	–15.2	–6.3
Wessex Formation (Lower Barremian)	NW of Cowleaze Chine, IOW *c.* 4 m below the White Rock [SZ 442 802]	MWH001a	Well-preserved micrite	–10.6	–2.9
		MWH001b	Well-preserved micrite	–10.5	–2.8
Upper Weald Clay (Lower Barremian)	Ockley Smokejacks Brickworks, Surrey *c.* 20 m below the Alford Sand member [TQ 1124 3755]	C145a	Well-preserved micrite	–12.5	–5.8
		C145b	Well-preserved micrite	–12.1	–6.0
		C145c	Well-preserved micrite	–11.7	–4.9

IOW, Isle of Wight; Sst, sandstone. For further locality information see Stewart (1981).

duplicated to ensure that quoted values are precise. Precision of the laboratory standard ($n = 18$) and the duplicates at UEA was in both cases better than $\pm 2\sigma$ 0.06‰ for δ^{13}C and $\pm 2\sigma$ 0.10‰ for δ^{18}O. At Oxford reproducibility of replicate analyses of standards was generally better than 0.1‰ for both δ^{13}C and δ^{18}O.

Results

Petrography and composition of Wealden calcrete nodules

The calcrete nodules collected from the Wessex Formation have sharp margins and are composed of a groundmass of non-ferroan dull-orange luminescing micrites or microspars with grey to orange body colours, depending on the quantity of Fe included (Fe has the effect of subduing luminescence). The groundmass contains variable quantities of silt to very fine sand grade detritus (quartz and feldspar); some nodules are pure micrite, while others are detrital grain rich, depending on the host substrate. Where detrital grains are present they appear to float in the groundmass (Fig. 3a) and many have corroded margins (Fig. 3b). This is well illustrated by cathodo-luminescence petrography where some grains are shown to be

enclosed by 10 μm thick haloes of bright-orange luminescing microspar that fills circumgranular cracks. In some areas of a nodule, 50–100 μm thick micritic grain coatings occur (Fig. 3a) and, more rarely, microspar coronas are also present. These coatings have dull-orange luminescence identical to that of the groundmass. Some nodules have vague structures of texturally denser carbonate within the groundmass, while 100–300 μm thick irregularly shaped former pores are spar filled. Most of the calcrete nodules are cut by spar-filled fractures (Fig. 3a), many of which are circumgranular and define micritic ped-like features (Fig. 3a) that range from 20 mm to 500 μm in diameter.

Fractures and circumgranular cracks (Fig. 4) are filled mainly by calcite cements formed in a characteristic order. The first stage of cementation is an isopachous fringe of non-ferroan dog-tooth calcite (Fig. 5a), typically 200–300 μm wide that sometimes completely infills fractures. Using CL, this stage of cementation is divisible into an early bright-orange-luminescing calcite with multiple thin layers of brighter and darker bands, followed by a dull brown, almost non-luminescent outer zone. The early bright-orange-luminescing cement has neomorphically altered the nodule substrate at
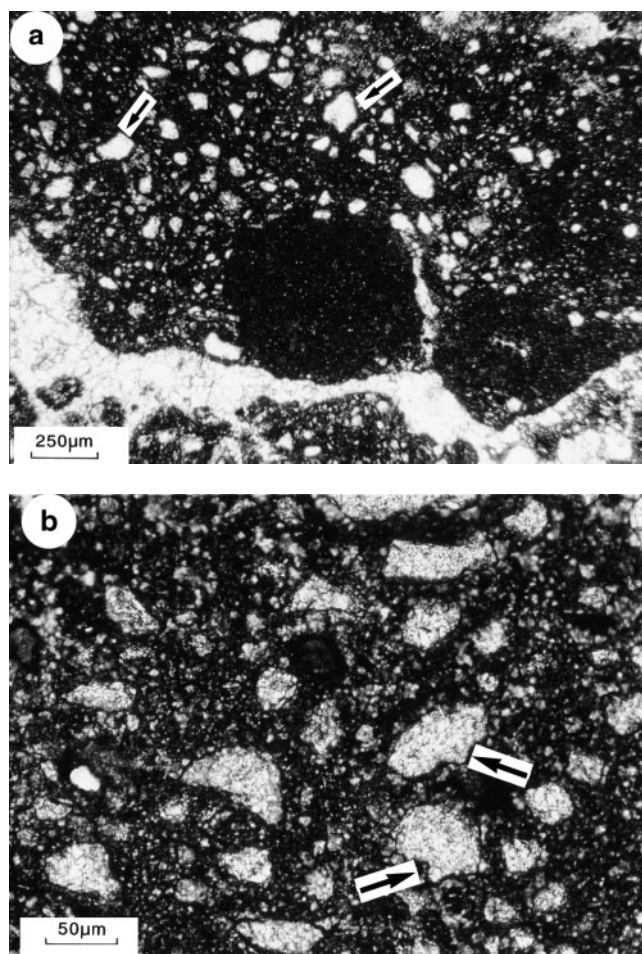
Fig. 3. (a) Plane-polarized-light photomicrograph of micritic calcrete nodule showing floating detrital grains (pale) and larger dark micritic peds (centre and bottom right). The peds are defined by spar-filled fractures (pale area toward base of photograph). The detrital grains have micritic coatings (arrows). Sample W3 from Brighstone Bay, Isle of Wight (see locality details in Table 1).
(b) Plane-polarized-light photomicrograph of floating detrital grains (light) with corroded margins. Clear embayments in the grains are arrowed. Sample W3 from Brighstone Bay, Isle of Wight (see locality details in Table 1).

crack margins. Where a number of fractures are close together, large zones (up to 8 mm wide) of the nodule have been altered (Fig. 4). These zones are easily recognized in hand specimen by 'bleached' areas adjacent to spar-filled fractures (Fig. 4). Using CL, the bleached zones can be identified by the bright-orange-luminescing cement between the groundmass of microspar crystals. This cement also fills cavities around corroded grains (described above).

In large fractures from within the Isle of Wight nodules, the non-ferroan calcite is followed by a blocky inclusion-rich ferroan calcite cement with patchy dull-brown luminescence. This cement most commonly occludes pore space, but in a few cases it is followed by pore-filling gypsum with bladed fabric. The Swanage samples have petrographically clear-ferroan calcite cements formed after the non-ferroan calcites.

The Weald Clay nodules are smaller concentrations of carbonate (2–20 mm diameter). The nodules still have sharp margins, but some are little more than peds (Fig. 5b) within

a dominantly clay matrix, itself with ped-like fabrics. The carbonates have broadly similar petrographic characteristics to those from the Wessex Formation, with cementation by non-ferroan and then clear ferroan calcite spars.

Stable isotope geochemistry

$\delta^{13}C$ values of well-preserved micrite (areas uncontaminated by bleaching) from the Wessex Formation calcretes have a mean of –10.2‰ and small range of *c.* 1.8‰ (Fig. 6; Tables 1 & 2), while $\delta^{18}O$ values have a mean of –4.0‰ and a range of 2.4‰ (Fig. 6; Tables 1 & 2). Mixed micrites (carbonate containing an unresolvable mixture of bleached and non-bleached micrite) from the Wessex Formation calcretes have an average $\delta^{13}C$ value of –9.9‰ and a mean $\delta^{18}O$ value of –3.7‰. Micrite data from the Weald Clay have a mean $\delta^{13}C$ of –12.1‰ (Fig. 6; Tables 1 & 2) and a mean $\delta^{18}O$ value of –5.6‰. Blocky ferroan calcite spars that fill fractures and vugs in the Wessex formation calcretes have a mean $\delta^{13}C$ of –15.0‰ and a mean $\delta^{18}O$ value of –6.3‰ (Fig. 6; Tables 1 & 2). Sample transects drilled across nodules, from areas of well-preserved micrite into bleached micrite at crack margins reveal up to 1.5‰ variability in $\delta^{13}C$ values (Fig. 7).

Interpretation of petrography and stable-isotope geochemistry

The sharp nodule margins (disorthic nodules of Wieder & Yaalon, 1974) are thought to result from churning within soils, displacing and rounding the nodules (pedoturbation). Shrinking and swelling of clay minerals during seasonal drying and wetting may have caused argillopedoturbation, and red mudstones in the Wessex Formation are known to contain up to 59% expandable clay in the clay fraction (Wright *et al.* 2000). Disorthic nodules are typical of vertisol soils (see discussion in Wright 1982).

Floating detrital grain texture, grain coronas and micritic coatings (cutans) are common, and diagnostic, calcrete fabrics (see review in Wright & Tucker 1991). Corroded grain margins show that matrix-replacive growth occurred, while a limited number of irregular open spaces suggests the presence of oversize pores also formed by displacive growth (Braithwaite 1989). The denser ped-like carbonate fabrics, and clear peds defined by circumgranular cracks were probably caused by strain in the soil matrix, induced by shrinkage and desiccation. This process was termed 'grainification' by Freytet & Plaziat (1982).

No evidence of post-pedogenic early diagenetic vadose-zone cementation was found. However, the presence of ferroan calcite cements with very negative $\delta^{13}C$ (see below) suggests that this calcite (and the preceding non-ferroan calcite) formed early during sediment burial close to sites of soil-zone organic-matter decomposition, possibly in a perched phreatic ground-water lens. It is possible that Fe^{2+}-rich reducing pore waters percolated downward from overlying siderite-bearing green-grey mudstones that were deposited in shallow floodplain lakes as described by Wright *et al.* (2000). The pore-filling gypsum might also be early diagenetic, sourced from the oxidation of pyrite. We regard only the clear ferroan calcite spars (Swanage and Ockley) as definite later burial cements. Identification of zones of bleached micrites close to fractures (Fig. 3) is important, as this has a bearing on the sampling and interpretation of some of the stable-isotopic data.
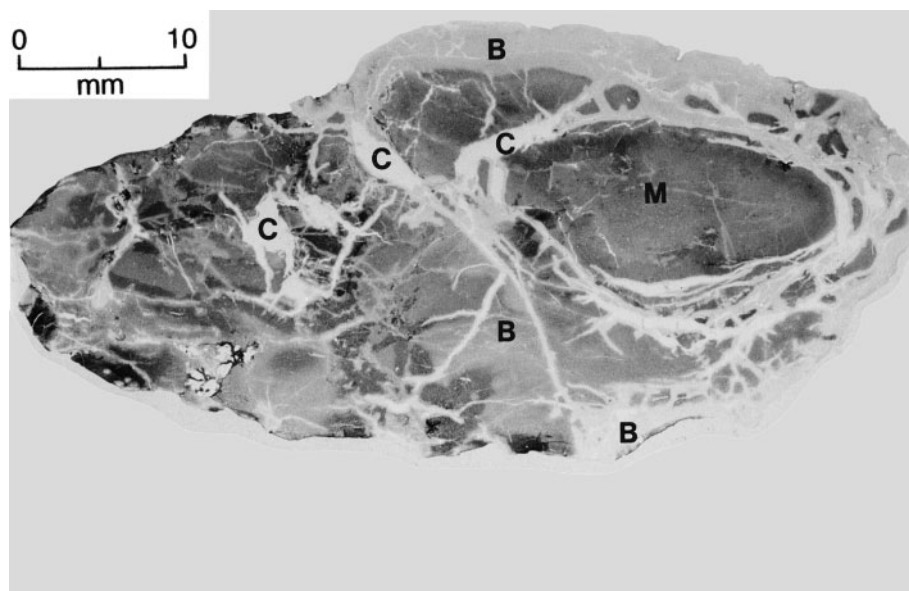
Fig. 4. Direct print from thin section of a complete calcrete nodule (sample GC103a, from the Wessex Formation on the Isle of Wight; see Table 1 for locality detail). The nodule is intensely brecciated and the cracks are now calcite cemented (C, see text for details). The darker portions of the nodule contain well-preserved micrite (M), while bleached areas (B) adjacent to cracks are mixed micrites. Only isotopic data from well-preserved micrites were used in pCO$_2$ calculations.

The δ^{18}O values for the Wessex Formation micrites are not particularly negative for calcretes and when considered with the negative δ^{13}C values (discussed below) plot close to the field of data for coastal soil carbonates identified by Cerling (1984). As discussed in Allen (1998), these δ^{18}O values suggest that the rainfall that fed soil moisture was relatively enriched in ^{18}O, consistent with a coastal floodplain setting under Mediterranean-type climatic conditions, with moisture sourced from nearby seawater (see also Anderson & Arthur 1983, pp.1–43). The Weald Clay samples have more typical negative δ^{18}O$_{(micrite)}$ values for calcretes, which might imply either more isotopically fractionated rainout, or less evaporation *in situ*. The latter possibility is consistent with a more waterlogged environment (Upper Weald Clay) compared with the seasonally flooded vertisol environments of the Wessex Formation (Wright *et al.* 2000).

The mean δ^{13}C value for the Wessex Formation calcretes (mean = $-10.2‰$) suggests that soil carbonate formed from C$_3$-dominated vegetation with low ingress of atmospheric carbon dioxide (Cerling 1984; and discussed in detail below). The Weald Clay samples, however, have more strongly negative values (mean = $-12.1‰$). These indicate a closed soil system with soil carbon dioxide sourced strongly from decaying organic matter. This is consistent with a partially waterlogged or low-permeability organic-rich clay, with positive gas out flux, preventing strong ingress of atmospheric CO$_2$. The soil carbonate may have formed at the margins of a vegetated swamp, which possibly generated methane (see further discussion below).

Comparison of the stable-isotope data from well-preserved micrite and mixed micrite shows only small differences (Fig. 6), although analysis of a single nodule shows maximum differences of up to 1.5‰ for δ^{13}C and about 1‰ for δ^{18}O (Fig. 7). For both isotopes, the bleached micrites generally have the least negative values. This implies that the early diagenetic non-ferroan cements have heavier isotopic compositions than the precursor micrites. The end-member isotopic compositions of these cements have not been precisely defined because the cement areas are smaller than our best present sampling resolution.

The negative δ^{18}O values for the ferroan calcite cements from the Wessex Formation are consistent with early burial cementation under meteoric-water-sourced phreatic conditions as demonstrated in numerous studies (see reviews in Hudson 1977; James & Choquette 1988). The very negative δ^{13}C values for these cements (Tables 1 & 2) imply a considerable input of isotopically light carbon from the oxidation of organic matter in the surrounding sediments (see also above).

Reconstruction of atmospheric pCO$_2$ from Wealden calcretes

In modern soils the δ^{13}C of soil carbonate is influenced by a variety of carbon sources, but principally by the proportion of C$_4$:C$_3$ plants in the overlying biomass (Cerling 1991). As C$_4$ plants probably did not evolve until the Miocene (Throughton *et al.* 1974), the pre-Miocene δ^{13}C of soil carbonate was presumably affected by two main inputs: atmospheric CO$_2$ and the production of CO$_2$ within the soil (by respiration and decay of C$_3$ organic matter). Modelling these parameters using diffusion equations, Cerling (1984, 1991) showed that at high atmospheric pCO$_2$, the δ^{13}C of soil carbonate becomes increasingly controlled by the isotopic composition of the atmospheric CO$_2$. This results in a positive correlation between increasing atmospheric pCO$_2$ and more positive calcrete δ^{13}C values.

Use of Cerling's (1991, 1992, 1999) model requires several assumptions and parameter estimates. Most critically, use of the model relies on the assumption that C$_4$ plants did not evolve until the Miocene (see discussions in Wright & Vanstone, 1991, and Kuypers *et al.*, 1999). In the present study, δ^{13}C data from fossil wood collected from the Wessex Formation, (Robinson & Hesselbo, unpublished data) are typically between –23‰ and –27‰, consistent with values expected for fossil C$_3$ vegetation (Bocherens *et al.* 1993). Data from the overlying Lower Greensand (Gröcke *et al.* 1999) have a similar range, indicating that the Early Cretaceous vegetation in question was dominantly of a C$_3$ type.
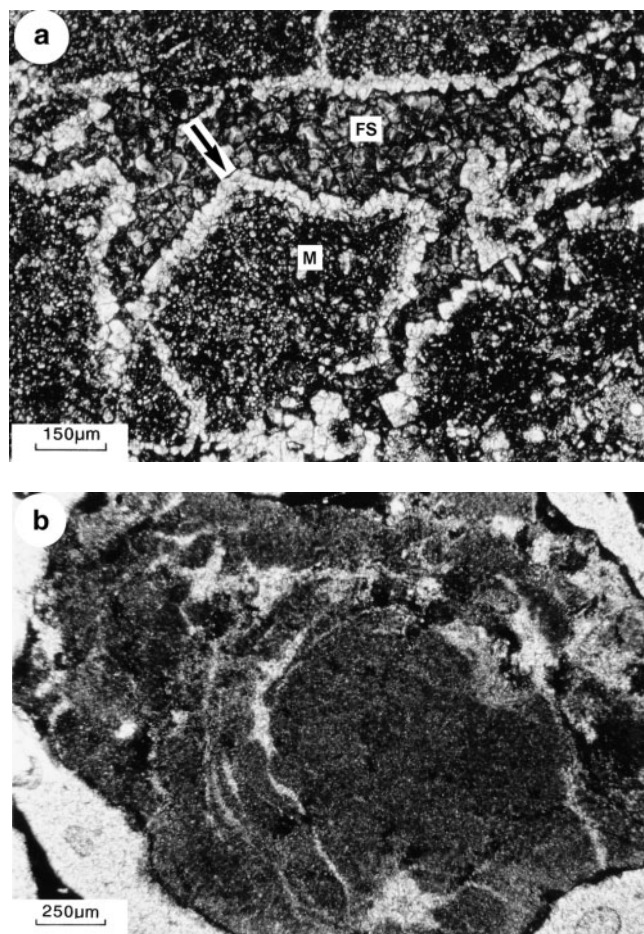
Fig. 5. (a) Plane-polarized-light photomicrograph showing micrite/microspar calcrete (M), isopachous fringe of non-ferroan dog-tooth calcite (arrow) and clear ferroan spar (FS) cementing a fracture. Sample 21999a from Swanage Bay, Dorset (see locality details in Table 1). (b) Plane-polarized-light photomicrograph showing non-ferroan micritic ped with clear circumgranular cracks. This ped is embedded in a clay matrix (not visible in the figure). Sample C145b from Ockley Smokejacks Brickworks, Surrey (see locality details in Table 1).
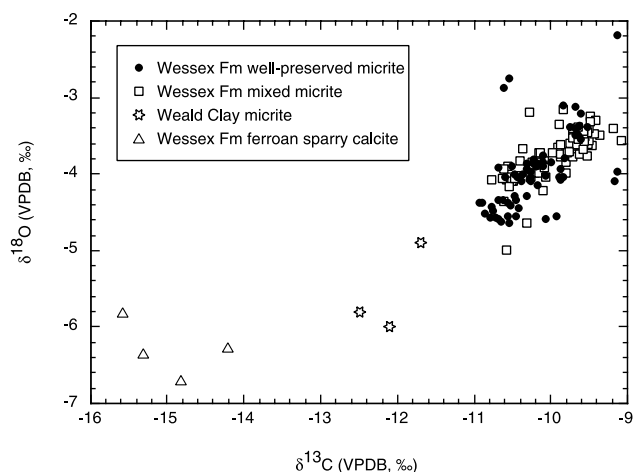

Fig. 6. Cross-plot of $\delta^{18}O$ against $\delta^{13}C$ showing all data discussed in the text.

Calcrete can form at a variety of depths within soil-profiles but the isotopic composition of soil carbonate is only constant below a depth of 0.2–0.3 m (Cerling 1991). The position of the Wessex Formation nodules within the soil profiles and the complete absence of rooted beds or exposure surfaces directly above the nodule forming horizons, suggests that these nodules formed at least 0.5 m below the soil-surface (cf. Wright *et al.* 2000). Given this depth of formation and the fact that the Wessex Formation calcrete nodules formed in semi-arid palaeosols, the nodules make promising candidates for reconstructing Early Cretaceous $p\mathrm{CO}_2$.

The Cerling model is most sensitive to the soil-respired component of CO_2 ($S_{(z)}$), which in soils that precipitate calcretes is typically between 5000 ppmV and 10 000 ppmV (Cerling 1991, 1992). The palaeosols of the Wessex Formation appear to have been seasonally flooded (Wright *et al.* 2000) and locally there are gleys and pseudo-gleys. This indicates that the $S_{(z)}$ of these soils was probably high (i.e. S(z)=10 000 ppmV) and representative of wetter soils (Cerling 1991).

The Cerling (1999) model was a modification of his 1992 model that incorporated a revised relationship between the $\delta^{13}\mathrm{C}$ of soil CO_2 and soil respired CO_2 (Davidson 1995), leading to the following equation:

$$C_a = \frac{S_{(z)}(\delta^{13}\mathrm{C}_s - 1.0044\delta^{13}\mathrm{C}_\phi - 4.4)}{\delta^{13}\mathrm{C}_a - \delta^{13}\mathrm{C}_s}$$

Where:
C_a = atmospheric $p\mathrm{CO}_2$
$S_{(z)}$ = CO_2 contributed by soil respiration (ppmV)
$\delta^{13}\mathrm{C}_s$ = isotopic composition of soil CO_2 (‰)
$\delta^{13}\mathrm{C}_\phi$ = isotopic composition of soil respired CO_2 (‰)
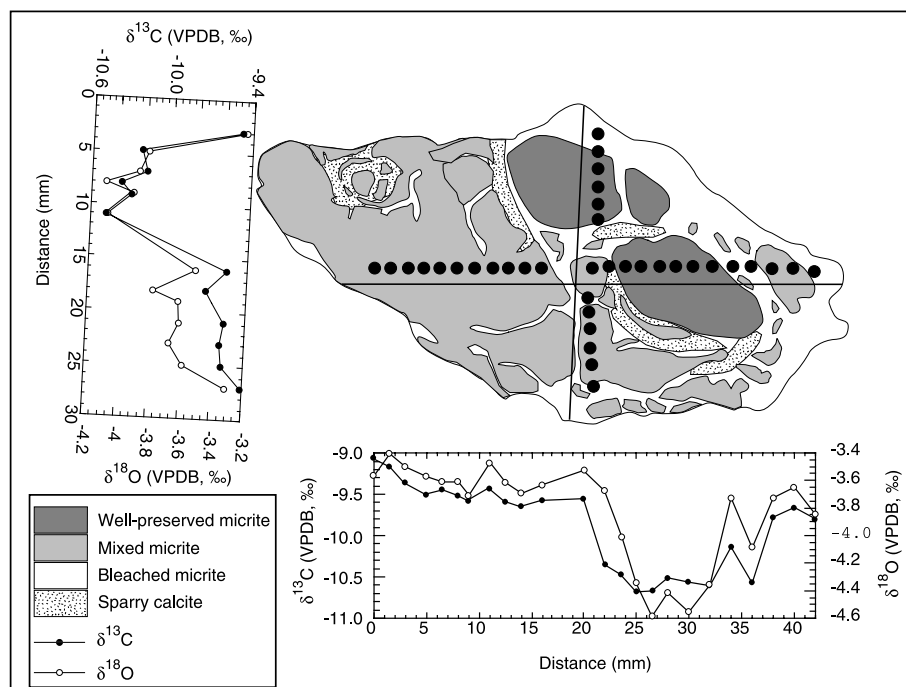$\delta^{13}\mathrm{C}_a$ = isotopic composition of atmospheric CO_2 (‰)

This equation was used by both Cerling (1999) and Ekart *et al.* (1999) to estimate atmospheric $p\mathrm{CO}_2$ change during the last 400 Ma. In the method of Ekart *et al.* (1999), the isotopic composition of atmospheric CO_2 was calculated by assuming a –8‰ fractionation between oceanic carbonate and atmosphere. These authors then used a –18‰ fractionation between $\delta^{13}\mathrm{C}_a$ and the carbon-isotopic composition of soil organic matter ($\delta^{13}\mathrm{C}_{(\mathrm{SOM})}$), and assumed that the $\delta^{13}\mathrm{C}_{(\mathrm{SOM})}$ had an identical isotopic composition to soil-respired CO_2 ($\delta^{13}\mathrm{C}_\phi$). Ekart *et al.* (1999) calculated the isotopic composition of soil CO_2 ($\delta^{13}\mathrm{C}_s$) from the isotopic composition of pedogenic carbonate using a fractionation factor of –8.98‰ (from Romanek *et al.* 1992) assuming a constant temperature of 25 ˚C.

Using the method of Ekart *et al.* (1999) and a $\delta^{13}\mathrm{C}$ value of Upper Hauterivian to Lower Barremian Tethyan shallow-marine carbonates of approximately 1.8‰ (Channell *et al.* 1993), we calculate a $\delta^{13}\mathrm{C}_a$ of –6.2‰ and a $\delta^{13}\mathrm{C}_{(\mathrm{SOM})}$ of –24.2‰. Using the average carbon-isotopic value for well-preserved Wessex Formation micrite (–10.2‰), we calculate a $\delta^{13}\mathrm{C}_s$ of –19.18‰. By substituting these values into the Cerling equation, we are able to estimate that atmospheric $p\mathrm{CO}_2$ was approximately 560 ppmV during the Early Barremian (using a preferred $S_{(z)}$ of 10 000 ppmV; Table 3). The model is most sensitive to changes in $S_{(z)}$ but there is also uncertainty associated with the $\delta^{13}\mathrm{C}$ of soil carbonate and hence we report this uncertainty to one standard deviation (Table 3).

In contrast to the Wessex Formation data, it is not possible to calculate an estimate of $p\mathrm{CO}_2$ for the Weald Clay data with an $S_{(z)}$ of 10 000 ppmV. This indicates that the concentration

Table 2. *Average $\delta^{13}C$ and $\delta^{18}O$ values for the various types of carbonate identified within Wealden calcrete nodules*

Lithostratigraphy	Carbonate type	Average δ^{13}C (VPDB, ‰)	Average δ^{18}O (VPDB, ‰)
Wessex Formation	Well-preserved micrite	−10.2	−4.0
Wessex Formation	Mixed micrite	−9.9	−3.7
Wessex Formation	Sparry calcite	−15.0	−6.3
Weald Clay	Well-preserved micrite	−12.1	−5.6

Fig. 7. Simplified sketch of GC103a showing two transects across the nodule and the variation in δ^{13}C and δ^{18}O.

Table 3. *Summary of the data necessary to use the model of Cerling (1999) and the method of Ekart et al. (1999); also summarized are the results of this method for the Wessex formation calcretes*

δ^{13}C (soil carbonate)	−10.2‰ (1σ = ±0.4)
δ^{13}C(surface ocean carbonate)	1.8‰
δ^{13}C$_a$	−6.2‰
δ^{13}C$_\phi$	−24.2‰
δ^{13}C$_s$	−19.18‰
Average atmospheric pCO$_2$ at $S_{(z)}$ = 5000 ppmV	279 ppmV
Average atmospheric pCO$_2$ at $S_{(z)}$ = 7000 ppmV	392 ppmV
Average atmospheric pCO$_2$ at $S_{(z)}$ = 10 000ppmV (Range of values at 1σ)	560 ppmV (244–895 ppmV)

The preferred value of $S_{(z)}$ is 10 000 ppmV.

of soil-respired CO$_2$ in the Weald Clay environment was probably higher than 10 000 ppmV (see also Royer *et al.* 2001), suggesting that the soils were marshy and waterlogged. These conditions would reduce the ingress of atmospheric CO$_2$ into the soil profile and hence make the data unsuitable for atmospheric pCO$_2$ reconstruction. This interpretation is entirely consistent with the suggestion that the Upper Weald Clay mainly represents lacustrine-lagoonal environments with waterlogged and swampy marginal areas (see Batten 1998; Allen 1998). The peds and other incipient calcrete nodules presumably formed on small topographic highs where some drying-out occurred.

Discussion

Using the model of Cerling (1999) and the method of Ekart *et al.* (1999) we estimate a maximum atmospheric pCO$_2$ for the Early Barremian of approximately 560 ppmV (about twice pre-industrial atmospheric level (PAL)). This result is consistent with estimates from a variety of other methods (Table 4). Ekart *et al.* (1999) published several estimates of atmospheric pCO$_2$ for the Late Jurassic and Cretaceous. The results of the present study and of Ekart *et al.* (1999) are shown in Figure 8 along with outputs from the geochemical models of Berner (1994), Tajika (1999) and Wallmann

Table 4. *Comparison of predicted Early Barremian atmospheric pCO_2 levels based upon a variety of methods*

Author	Estimated level of atmospheric pCO_2	Source
This study	*c.* 560 ppmV (*c.* 2 times PAL)	Palaeosol carbonate and the model of Cerling (1999) and method of Ekart *et al.* (1999)
Berner (1994)	*c.* 960 ppmV (*c.* 3.5 times PAL)	Geochemical model based on the long term carbon cycle
Tajika (1999)	*c.* 825 ppmV (*c.* 3 times PAL)	Biogeochemical model that incorporates elements of the short term carbon cycle (i.e. short term carbon burial)
Wallmann (2001)	*c.* 600–700 ppmV (*c.* 2.2–2.5 times PAL)	Biogeochemical model that incorporates elements of the short term carbon cycle (i.e. short-term carbon burial)

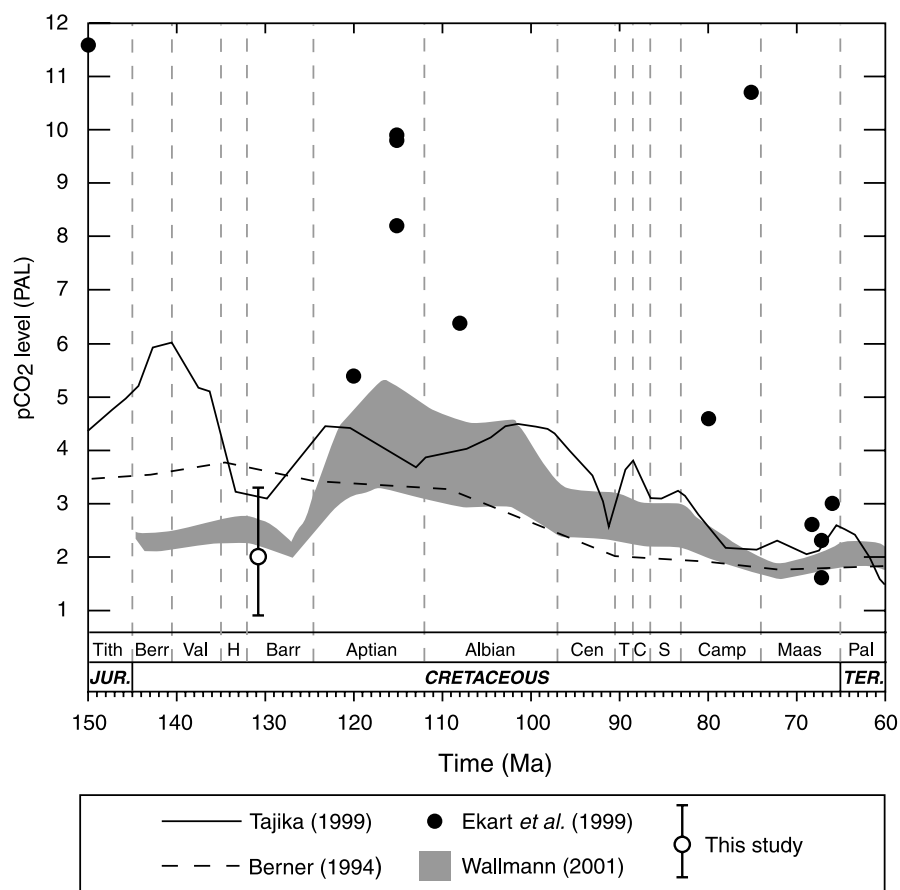Pre-industrial atmospheric level (PAL) is taken to be *c.* 275 ppmV.

Fig. 8. Atmospheric pCO_2 change through the Cretaceous as inferred from biogeochemical models (Berner 1994: Tajika 1999; Wallmann 2001) and from soil carbonate (Ekart *et al.* 1999). The result of the present study (at an $S_{(z)}$ of 10 000 ppmV) is shown by a unfilled circle. The error bars represent 1 standard deviation of uncertainty. All data have been plotted on the time scale of Harland *et al.* (1990) for consistency with previous studies. Use of other time scales does not alter the observed trends in pCO_2 but does alter the apparent rates of change. Pre-industrial atmospheric pCO_2 level (PAL) is taken to be *c.* 275 ppmV.

(2001). When compared with the results of Ekart *et al.* (1999) our data suggest that there was a low in atmospheric pCO_2 around the Early Barremian. Similarly low atmospheric pCO_2 levels were not reached again until the latest Cretaceous. These relatively short term pCO_2 changes are missed by global scale models such as GeoCARB II (Berner 1994) because the data input scales are of low resolution (every ten million years in the Cretaceous of GeoCARB II). As identified by Royer *et al.* (2001), a combined modeling and proxy approach will be the most informative. There are many reasons why atmospheric pCO_2 lows can occur, such as long term burial of organic carbon or decreased volcanism (e.g. Jenkyns 1999).

The low in pCO_2 cannot be precisely dated due to the currently rather poor chronostratigraphic resolution for the palaeosol data. Interestingly, however, a similar low in atmospheric pCO_2 has been predicted by some geochemical models (Tajika 1999; Wallmann 2001; see Fig. 8), and attributed to a

decrease in global magma eruption rate. This result runs counter to previous modelled predictions that atmospheric pCO_2 simply declined during the Early Cretaceous (Berner 1994; Ekart *et al.*1999; Fig. 8).

It has been generally thought that changes in atmospheric pCO_2 levels are the cause of climatic change (e.g. Barron & Washington 1985). Recently, however, this interpretation has been challenged (Veizer *et al.* 2000) based upon a comparison of temperature records with the predicted atmospheric pCO_2 levels of Berner (1994). Veizer *et al.* (2000) found discrepancies between measured palaeotemperatures and predicted temperatures from atmospheric pCO_2 forcing during the Late Jurassic and Early Cretaceous. On the basis of geological (Frakes & Francis 1988) and isotopic evidence (Douglas & Savin 1975; Frakes *et al.* 1994; Frakes 1999), the early Cretaceous (Berriasian–Barremian) is thought to have been relatively cooler than the mid-Cretaceous greenhouse, which may have been initiated in the Late Barremian to Early Aptian (Larson

1991a, b; Larson & Erba 1999). The relatively low atmospheric pCO$_2$ levels predicted by our data are consistent with these suggestions of cooler palaeoclimates in the Early Barremian (relative to the mid-Cretaceous) therefore supporting the link between palaeo-pCO$_2$ and palaeotemperature. Undoubtedly as more data from palaeosol carbonates are published, so the complexity of our understanding of atmospheric pCO$_2$ change and the implications for palaeoclimate during the Cretaceous will increase.

Conclusions

(1) Petrographic evidence suggests that the small soil-carbonate nodules of the Wessex Formation resulted from pedogenic processes within semi-arid vertisols.

(2) The nodules show evidence of several periods of cementation, each isotopically distinct, although in some cases there are only small differences in the isotopic values of bleached and well-preserved micrite. With improved micro-sampling techniques it may be possible to refine the broad isotopic groups identified here.

(3) Our data from the Weald Clay cannot be used to predict atmospheric pCO$_2$ levels using the Cerling model. This is probably because the Weald Clay environment was marshy and waterlogged. Careful consideration of palaeoenvironment is obviously necessary prior to any atmospheric pCO$_2$ reconstruction using Cerling's models.

(4) Using well-preserved-micrite data from the Wessex Formation nodules, the model of Cerling (1999) and the method of Ekart et $al.$ (1999) we predict an atmospheric pCO$_2$ level of approximately 560 ppmV for the Early Barremian.

(5) Some previous studies of atmospheric pCO$_2$ levels during the Cretaceous have suggested that values were relatively higher at the Jurassic–Cretaceous boundary and fell steadily through the Early Cretaceous (cf. Berner 1994; Ekart et $al.$ 1999). However, our data suggest that atmospheric pCO$_2$ levels were low during the mid-Early Cretaceous before rising to the high levels of the mid-Cretaceous 'greenhouse'. The pCO$_2$ levels in the Early Barremian may be comparable with those levels predicted for the latest Maastrichtian.

References

ALLEN, P. 1975. The Wealden of the Weald: a new model. $Proceedings$ of the $Geologists'$ $Association$, **86**, 389–437.
ALLEN, P. 1981. Pursuit of Wealden Models. $Journal$ of the $Geological$ $Society,$ $London$, **138**, 375–405.
ALLEN, P. 1998. Purbeck-Wealden (Early Cretaceous) climates. $Proceedings$ of the $Geologists'$ $Association$, **109**, 197–236.
ALLEN, P. & WIMBLEDON, W.A. 1991. Correlation of NW European Purbeck-Wealden (non-marine Lower Cretaceous) as seen from the English type-areas. $Cretaceous$ $Research$, **12**, 511–526.
ANDERSON, T.F. & ARTHUR, M.A. 1983. Stable isotopes of oxygen and carbon and their application to sedimentological and paleoenvironmental prob-

lems. $In:$ ARTHUR, M.A. (ed.) $Stable$ $isotopes$ in $sedimentary$ $geology$. SEPM short courses, **10**, 1–151.
ANDREWS, J.E., TANDON, S.K. & DENNIS, P.F. 1995. Concentration of carbon dioxide in the Late Cretaceous atmosphere. $Journal$ of the $Geological$ $Society,$ $London$, **152**, 1–3.
ARKELL, W.J. 1947. The $Geology$ of the $Country$ $around$ $Weymouth,$ $Swanage,$ $Corfe$ and $Lulworth$. HMSO.
BARRON, E.J. & WASHINGTON, W.M. 1985. Warm Cretaceous Climates: High Atmospheric CO$_2$ as a Plausible Mechanism. $In:$ SUNDQUIST, E.T. & BROECKER, W.S. (eds) The $Carbon$ $Cycle$ and $Atmospheric$ $CO_2:$ $Natural$ $Variations$ $Archean$ to $Present$. American Geophysical Union, Geophysical Monographs, **32**, 546–553.
BATTEN, D.J. 1998. Palaeoenvionmental implications of plant, insect and other organic-walled microfossils in the Weald Clay Formation (Lower Cretaceous) of south east England. $Cretaceous$ $Research$, **19**, 279–315.
BERNER, R.A. 1991. A model for atmospheric CO$_2$ over Phanerozoic time. $American$ $Journal$ of $Science$, **291**, 339–376.
BERNER, R.A. 1994. GEOCARB II: a revised model of atmospheric CO$_2$ over Phanerozoic time. $American$ $Journal$ of $Science$, **294**, 56–91.
BOCHERENS, H., FRIIS, E.M., MARIOTTI, A. & PEDERSEN, K.R. 1993. Carbon isotopic abundances in Mesozoic and Cenozoic fossil plants: palaeoecological implications. $Lethaia$, **26**, 347–358.
BRAITHWAITE, C.J.R. 1989. Displacive calcite and grain breakage in sandstones. $Journal$ of $Sedimentary$ $Petrology$, **59**, 258–266.
CERLING, T.E. 1984. The stable isotopic composition of modern soil carbonate and its relationship to climate. $Earth$ and $Planetary$ $Science$ $Letters$, **71**, 229–240.
CERLING, T.E. 1991. Carbon dioxide in the atmosphere: evidence from Cenozoic and Mesozoic paleosols. $American$ $Journal$ of $Science$, **291**, 377–400.
CERLING, T.E. 1992. Use of carbon isotopes in paleosols as an indicator of the p(CO2) of the paleoatmosphere. $Global$ $Biogeochemical$ $Cycles$, **6**, 307–314.
CERLING, T.E. 1999. Stable carbon isotopes in palaeosol carbonates. $In:$ THIRY, M. & SIMM-COINÇON, R. (eds)$Palaeoweathering,$ $palaeosurfaces$ and $related$ $continental$ $deposits$. Special Publication of the International Association of Sedimentologists, **27**, 43–60.
CHANNELL, J.E.T., ERBA, E. & LINI, A. 1993. Magnetostratigraphic calibration of the Late Valanginian carbon isotope event in pelagic limestones from Northern Italy and Switzerland. $Earth$ and $Planetary$ $Science$ $Letters$, **118**, 145–166.
COPLEN, T.B. 1994. Reporting of stable hydrogen, carbon and oxygen isotopic abundances. $Pure$ and $Applied$ $Chemistry$, **66**, 273–276.
DAVIDSON, G.R. 1995. The stable isotopic composition and measurement of carbon in soil CO2. $Geochemica$ et $Cosmochimica$ $Acta$, **59**, 2485–2489.
DICKSON, J.A.D. 1965. A modified staining technique for carbonates in thin section. $Nature$, **205**, 587.
DOUGLAS, R.G. & SAVIN, S.M. 1975. Oxygen and carbon isotope analyses of Tertiary and Cretaceous microfossils from Shatsky Rise and other sites in the North Pacific Ocean. $Initial$ $Reports$ of the $Deep$ Sea $Drilling$ $Project$, **32**, 509–520.
EKART, D.D., CERLING, T.E., MONTAÑEZ, I.P. & TABOR, N.J. 1999. A 400 million year carbon isotope record of pedogenic carbonate: implications for paleoatmospheric carbon dioxide. $American$ $Journal$ of $Science$, **299**, 805–827.
FRAKES, L.A. 1999. Estimating the global thermal state from Cretaceous sea surface and continental temperature data. $In:$ BARRERA, E. & JOHNSON, C.C. (eds) $Evolution$ of the $Cretaceous$ $Ocean-Climate$ $System$. Geological Society of America, Special Papers, **332**, 49–57.
FRAKES, L.A. & FRANCIS, J.E. 1988. A guide to Phanerozoic cold polar climates from high-latitude ice-rafting in the Cretaceous. $Nature$, **333**, 547–549.
FRAKES, L.A., PROBST, J.-L. & LUDWIG, W. 1994. Latitudinal distribution of paleotemperature on land and sea from early Cretaceous to middle Miocene. $Comptes$ $Rendus,$ $Academie$ $Science,$ $Paris,$ $Serie$ II **318**, 1209–1218.
FREYTET, P. & PLAZIAT, J.C. 1982. Continental carbonate sedimentation and pedogenesis – Late Cretaceous and Early Tertiary of southern France. $Contributions$ to $Sedimentology$, **12**, 1–213.
GRÖCKE, D.R., HESSELBO, S.P. & JENKYNS, H.C. 1999. Carbon-isotope composition of Lower Cretaceous fossil wood: Ocean-atmosphere chemistry and relation to sea-level change. $Geology$, **27**, 155–158.
HARLAND, W.B., ARMSTRONG, R.L., COX, A.V., CRAIG, L.E., SMITH, A.G. & SMITH, D.G. 1990. A $geologic$ $time$ $scale$ 1989. geologic time scale Cambridge University, Cambridge University Press.
HASEGAWA, T. 1997. Cenomanian–Turonian carbon isotope events recorded in terrestrial organic matter from northern Japan. $Palaeogeography,$ $Palaeoclimatology,$ $Palaeoecology$, **130**, 251–273.
HUDSON, J.D. 1977. Stable isotopes and limestone lithification. $Journal$ of the $Geological$ $Society$ of $London$, **133**, 637–660.
HUGHES, N.F. & CROXTON, C.A. 1973. Palynological correlation of the Dorset "Wealden". $Palaeontology$, **16**, 567–601.
JAMES, N.P. & CHOQUETTE, P.W. (eds) 1988. $Palaeokarst$. Springer-Verlag, New York.
JENKYNS, H.C. 1999. Mesozoic anoxic events and palaeoclimate. $Zentralblatt$ $Geologie$ und $Paläontologie$, **1997**, 943–949.

JONES, C.E. & JENKYNS, H.C. 2001. Seawater strontium isotopes, oceanic anoxic events, and seafloor hydrothermal activity in the Jurassic and Cretaceous. *American Journal of Science*, **301**, 112–149.

KUYPERS, M.M.M., PANCOST, R.D. & SINNINGHE-DAMSTE, J.S. 1999. A large and abrupt fall in atmospheric CO_2 concentration during Cretaceous times. *Nature*, **399**, 342–345.

LARSON, R.L. 1991*a*. Latest pulse of Earth: Evidence for a mid-Cretaceous superplume. *Geology*, **19**, 547–550.

LARSON, R.L. 1991*b*. Geological consequences of superplumes. *Geology*, **19**, 963–966.

LARSON, R.L. & ERBA, E. 1999. Onset of the mid-Cretaceous greenhouse in the Barremian–Aptian: Igneous events and the biological, sedimentary and geochemical responses. *Paleoceanography*, **14**, 663–678.

LINI, A., WEISSERT, H. & ERBA, E. 1992. The Valanginian carbon isotope event: a first episode of greenhouse climate conditions during the Cretaceous. *Terra Nova*, **4**, 374–384.

MENEGATTI, A.P., WEISSERT, H., BROWN, R.S., TYSON, R.V., FARRIMOND, P., STRASSER, A. & CARON, M. 1998. High-resolution (δ^{13}C) stratigraphy through the early Aptian "Livello Selli" of the Alpine Tethys. *Paleoceanography*, **13**, 530–545.

MORA, C.I., DREISE, S.G. & COLARUSSO, L.A. 1996. Middle to Late Palaeozoic Atmospheric CO_2 Levels from Soil Carbonate and Organic Matter. *Science*, **271**, 1105–1107.

OLDHAM, T.C.B. 1976. Flora of the Wealden plant debris beds of England. *Palaeontology*, **19**, 437–502.

ROMANEK, C.S., GROSSMAN, E.L. & MORSE, J.W. 1992. Carbon isotopic fractionation in synthetic aragonite and calcite: Effects of temperature and precipitation rate. *Geochemica et Cosmochimica Acta*, **56**, 419–430.

ROYER, D.L., BERNER, R.A. & BEERLING, D.J. 2001. Phanerozoic atmospheric CO_2 change: evaluating geochemical and paleobiological approaches. *Earth-Science Reviews*, **54**, 349–392.

SPICER, R.A. & CORFIELD, R.M. 1992. A review of terrestrial and marine climates in the Cretaceous with implications for modelling the 'Greenhouse Earth'. *Geological Magazine*, **129**, 169–180.

STEWART, D.J. 1981. A field guide to the Wealden Group of the Hastings area and the Isle of Wight. *In:* ELLIOT, T. (ed.) *Field guides to modern and ancient fluvial systems in Britain and Spain.* International Fluvial Conference, University of Keele, 3.1–3.32.

TAJIKA, E. 1999. Carbon cycle and climate change during the Cretaceous inferred from a biogeochemical carbon cycle model. *The Island Arc*, **8**, 293–303.

THROUGHTON, J.H., WELLS, P.V. & MOONEY, H.A. 1974. Photosynthetic mechanisms in ancient C_4 and CAM species. *Carnegie Institution of Washington Yearbook*, **73**, 812–816.

VEIZER, J., GODDERIS, Y. & FRANCOIS, L.M. 2000. Evidence for decoupling of atmospheric CO_2 and global climate during the Phanerozoic eon. *Nature*, **408**, 698–701.

WALLMANN, K. 2001. Controls on the Cretaceous and Cenozoic evolution of seawater composition, atmospheric CO_2 and climate. *Geochemica et Cosmochimica Acta*, **18**, 3005–3025.

WEISSERT, H. & BRÉHÉRET, J.-G. 1991. A carbonate carbon-isotope record from Aptian-Albian sediments of the Vocontian trough (SE France). *Bulletin de la Société Géologique de France*, **162**, 1133–1140.

WIEDER, M. & YAALON, D.H. 1974. Effect of matrix composition on carbonate nodule crystallisation. *Geoderma*, **11**, 95–121.

WRIGHT, V.P. 1982. Calcrete palaeosols from the lower Carboniferous Llanelly Formation. *South Wales. Sedimentary Geology*, **33**, 1–33.

WRIGHT, V.P., TAYLOR, K.G. & BECK, V.H. 2000. The paleohydrology of Lower Cretaceous seasonal wetlands, Isle of Wight, southern England. *Journal of Sedimentary Research*, **70**, 619–632.

WRIGHT, V.P. & TUCKER, M.E. (eds) 1991. *Calcretes.* Blackwell Scientific Publications, Oxford.

WRIGHT, V.P. & VANSTONE, S.D. 1991. Assessing the carbon dioxide content of ancient atmospheres using palaeocalcretes: theoretical and empirical constraints. *Journal of the Geological Society, London*, **148**, 945–947.